Polish Journal of Medical Physics and Engineering
The Journal of Polish Society of Medical Physics
ISSN 1898-0309, doi: 10.2478/pjmpe-2024-0027

December 2024
Vol 30, Issue 4

Scientific Paper

Bionic model of blood cell segmentation based on impulse image transformation

Roman Yu. BUKHTIIAROV[1,AEF,*], Anatoliy V. TARASOV[2,BDF], Andriy V. RABOTIAHOV[3,CEF], Victor M. CHEVERDA[4,DEF], Alexander GIGOLAEV[5,BDF]

[1]*LTD "Bionic Intelligent Systems", Kyiv, Ukraine*
[2]*Department of Research and Development, LTD "Bionic Intelligent Systems", Kyiv, Ukraine*
[3]*Department of Research, Kharkiv National University of Radio Electronics, Kharkiv, Ukraine*
[4]*Communal Non-Commercial Enterprise of Merefa City Council "Merefian Central District Hospital", Merefa, Ukraine*
[5]*Department of Research, LTD "Bionic Intelligent Systems", Kyiv, Ukraine*
[*]*Corresponding author: Roman Yu. Bukhtiiarov; roman.yuu@ukr.net*

(received 20 March 2024; revised 25 June and 19 August 2024; accepted 28 September 2024)

Abstract

Introduction: The relevance of the proposed topic is determined by the high incidence of hematopoietic system diseases and the lack of a clear understanding at the cytological level of their mechanisms and correction methods. The purpose of the article is to create images of blood cells using mathematical modelling.

Materials and Methods: To achieve the defined goal, fundamental research methods were utilized, among which the method of mathematical modelling played a significant role, employed in creating a bionic model of blood cells.

Results: The results of this study have indicated that the task of recognizing blood cells in complex images poses a significant challenge in the field of medicine. Such tasks are complicated by the transparency of cells compared to the buffer solution, uneven thickness of the blood smear, and varying staining of the smear. Therefore, there is a need to improve the segmentation algorithm of the bionic model and develop new, more efficient methods and models for image recognition. The algorithm for constructing the bionic model segmentation consists of four main steps.

Conclusion: The practical significance of this research lies in the possibility of using the obtained results in the further development of clinical correction and treatment methods for diseases such as anaemia, thrombocytopenia, and neoplastic processes.

Keywords: haematology; immunological reactions; biotechnology; physical phenomena; haemodynamics.

Introduction

The problem of object recognition using modern technologies remains relevant in scientific circles. For instance, in the field of medical diagnostics, there is an increasing trend to apply advanced technical devices, methods, and models where the quality of diagnosis directly depends on the quality of indicators obtained through object recognition in diagnostics. Since several researchers focused on related topics and obtained somewhat isolated and fragmented data, the presented theme can be considered relevant. Furthermore, practically all researchers whose works were considered mostly explored the forms of blood components and their membranes, also drawing parallels with similar studies on stem cells. However, none of the authors illuminated the specifics of the blood cell segmentation process through modelling. According to O. Kuzomin et al.[1] most data analysis tools use two main technologies: machine learning and visualization (presentation of data in visual form).

The quality of visualization is determined by the ability of graphical data representation. Changes in the graphical presentation, such as colour and shape variations, help identify hidden dependencies. This applies to the recognition of objects in the form of their video images and, specifically, the segmentation of blood cells in an image. As noted by A.T. Abu-Jassar et al.[2] the widespread use of multimedia systems is explained by several advantages, including the simplicity and convenience of multimedia system interfaces, making them easy to use; the ability to store a large volume of diverse information on a single medium, allowing the storage and transmission of various types of data; the ability to compare and process images using different programs and tools, expanding their processing and analysis capabilities.

Authors' contribution:
A – Research concept and design, B – Collection and/or assembly of data, C – Data analysis and interpretation, D – Writing the article, E – Critical revision of the article, F – Final approval of the article.

According to A.V. Markushevska and M.O. Savchenko[3], O.M. Morozova et al.[4] in the laminar flow of blood containing blood cells, internal layers behave quite organized. Each layer of fluid hinders the movement of the adjacent layer closer to the central axis of the vessel. In the studies by L.V. Batyuk and N.M. Kizilova[5], V.V. Novytskyy and V.V. Novytskyy Jr.[6] it was found that the oscillation of erythrocyte membranes during their movement is related to the glucose level in the blood, significantly affecting the dielectric and electrical characteristics of erythrocytes. The significance of membrane elasticity has long been discussed in terms of practical applications. However, in recent years, it has become apparent that membrane viscosity is a critical aspect for accurately reproducing the membrane relaxation time under the influence of external stimuli.

In another work, L.V. Batyuk and N.M. Kizilova[7] describe laminar blood flows, suspensions of blood erythrocytes, or shadows of erythrocytes in a physiological solution through cylindrical tubes of circular cross-section, simulating vessels. However, the authors do not explain changes in the shape or membranes of red blood cells. O.V. Pertsov and V.P. Berest[8], in their study, used modelling of reversible platelet aggregation by directly considering cell inactivation using temporal dependence and adjusting the deaggregation term. However, the scientists did not consider the shape and morphological features of platelets. B. Cao et al.[9] emphasize that the proposed approach utilizes all available information related to the target modality from various sources to create any missing modality within one model. Nevertheless, the positive trend and prospects for the increased use of technical devices for qualitative diagnostics are restrained by the insufficient efficiency of the theoretical, scientific side of this problem, which ensures the necessary quality of recognition.

Each of these components performs crucial functions in the body, such as transporting oxygen and nutrients, immune reactions, and blood clotting processes. The scientific aspect is characterized by a series of limitations in the theories underlying the methods and models of image recognition technical devices, which, naturally, affects their practical application. Regarding blood cell recognition, these reasons include: the overlay of one cell on another, variation in geometric cell sizes, low contrast of images, variability in the staining of blood smears, different colour schemes in images, errors in object contour highlighting, and the influence of noise and non-target objects, which can distort images. According to B.C. Ko et al.[10] these circumstances lead to the need for developing new, more effective methods and models of image recognition, the application of which will contribute to eliminating the specified reasons and improving the quality of recognition.

A. Shah et al.[11] summarizes advancements in the automated diagnosis of leukemia using machine learning and image processing. It highlights significant progress in developing automated systems, which can reduce errors and increase diagnostic speed. Challenges include the need for large annotated datasets and image quality variability, suggesting future research areas.

K.T. Navya et al.[12] reviews methods for analyzing RBCs from PBS images to detect anemia, categorizing approaches into RBC segmentation, classification, and anemia detection. It emphasizes the necessity for automated, robust, and cost-effective techniques due to the limitations of manual analysis, highlighting advancements in image processing but indicating a need for further research to enhance accuracy and reliability.

A. Basu et al.[13] reviews recent trends in deep learning for nucleus segmentation in histopathology images, focusing on developments from 2017 to 2021. It discusses various deep learning models, noting improvements in accuracy and efficiency. Challenges include handling overlapping regions and variability in images, with future research needed to enhance model robustness.

Current research in blood component image analysis reveals significant gaps, including the lack of comprehensive segmentation models, the need for large annotated datasets and improved image quality, and the challenges in transitioning from manual to automated analysis techniques. Deep learning faces issues with overlapping regions and image variability, and there is a disconnect between theoretical models and practical applications. Despite these gaps, notable contributions include advancements in automated leukemia diagnosis, comprehensive reviews of RBC analysis methods, and surveys of deep learning trends, all highlighting progress and suggesting future research directions to enhance diagnostic accuracy and efficiency.

Thus, the bionic blood model promises to revolutionize medical practice and the development of biotechnology by providing the ability to create synthetic blood analogues with many advantages, including the absence of the risk of infection transmission, contamination, and storage limitations.

The research aims to develop an algorithm that both creates images of blood components and segments them. This involves not only generating accurate images of blood cells but also implementing effective methods for segmenting different types of cells. The task of the work is to explain the morphological changes of cells based on cytological element models; explain the features of the segmentation of erythrocytes, leukocytes, and platelets.

Materials and Methods

To achieve the set goal, fundamental research methods were employed: cytological method, mathematical modelling method, which serves as the basis for creating a bionic model of blood cells, image processing methods, and models including energy methods (methods of the so-called active contour), threshold segmentation methods, methods of homogeneous region extraction, clustering methods, segment boundary extraction methods, and combinatorial methods. For processing contemporary scientific literature, analysis, and synthesis methods were used. The object of the research is the

phenomenon of blood cell segmentation, and the subject of the research is the blood components themselves. The use of mathematical modelling allows avoiding the need to create large physical models that require material costs, accelerating the process of determining characteristics (especially when using computer technologies and efficient computational methods and algorithms). The investigation of the modelling object and the creation of its mathematical description included establishing relationships between various characteristics of the process, determining boundary and initial conditions, and formalizing the process in the form of a system of mathematical relationships. This approach allowed understanding and describing the dynamics of the modelling object using mathematical equations. To obtain research results, the following were used: the Weber-Fechner law, the Somjen sensory coding effect, and for calculations, the Dice, Sorensen, and Cekanovskii similarity coefficients. The validation of the bionic model was performed on cytological material, using a randomized sample of 50 individuals.

Cytological material was collected from 50 participants by obtaining 3-4 blood smears on slides from each respondent. Using an automated microscopy hardware-software complex, images of blood cells were created. The images for the analysis were obtained from an open medical image database created through the cooperation of several leading universities and medical institutions. This database contains high-quality images of blood smears that were captured using modern automated microscopes. Each image included from 2000 to 3000 cells, which ensured the representativeness and accuracy of the analysis. The use of such a database ensured high reliability and validity of the study results.

Blood cell images were subjected to automatic segmentation using the bionic model. This means that the model identified individual cells in the images. A visual quality control of segmentation was conducted by an operator specialist. The operator removed any incorrectly segmented cells or images. The Dice Similarity Coefficient (DSC) metric was used to evaluate the quality of segmentation, helping to determine how well the segmentation results corresponded to reality. The following formulas were used for calculations:

$$g_{i,j}^{1} = \frac{1}{T}\sum_{i}^{i+T} a_{i,j} \qquad \text{Eq .1}$$

This formula (**Equation 1**) calculates the average value of a pixel's color component (RGB) over a specific interval *T*. Here, $a_{(i,j)}$ represents the value of the pixel's color component (e.g., red, green, or blue), *i* and *j* are the pixel's coordinates, and *T* is the analysis interval that determines how many neighboring pixels are considered in calculating the average value.

$$g_{i,j}^{2} = max^{*}(g^{1}) - max(g_{i}^{1}) + g_{i,j}^{1} \qquad \text{Eq. 2}$$

This formula (**Equation 2**) calculates an adjusted value of the pixel's color component, where $\max^{*}(g^{1})$ is the maximum value among all color components in all images, and $\max(g_i^1)$ is the maximum value within the same row of the image. This adjustment helps in normalizing the pixel color values across different images and ensuring consistency in subsequent processing steps.

$$g_{i,j}^{3} = \frac{1}{T}\sum_{i}^{i+T} g_{i,j}^{2} \qquad \text{Eq. 3}$$

where: $a_{i,j}$ – value that constitutes the RGB colour of the pixel; *i=0/(l – T – 1)*, *l* – length of the image row; *j=0/(h – 1)*, *h* – length of the image column; *T* – analysis interval; *T=6/14*, $max^{*}(g^{1})$ – maximum value g^{1}on all images; $g_{i,j}^{1}\ max(g_{i}^{1})$ – maximum values g^{1}in a row. This formula (**Equation 3**) computes the average of the adjusted pixel color values over the interval *T*. The purpose is to smooth the color variations and prepare the image for further analysis, ensuring that the important features of the image are retained while reducing noise.

$$d = max^{r,g,b}(g^{3}) - min^{r,g,b}(g^{3}) \qquad \text{Eq. 4}$$

This formula (**Equation 4**) calculates the difference between the maximum and minimum values of the RGB color components across all images. This difference, d, highlights the contrast between the colors, which is crucial for detecting edges and boundaries within the image.

$$d_{i,j}^{1} = \begin{cases} 1, & max^{r,g,b}(g_{i,j}^{3}) < \frac{d}{2} \\ 0, & max^{r,g,b}(g_{i,j}^{3}) \geq \frac{d}{2} \end{cases} \qquad \text{Eq. 5}$$

where: *i=0/(l–1)*, *l* – length of the row of the image; *j=0/(h–1)*, *h* – length of the column of the image; $max^{r,g,b}(g^{3})/min^{r,g,b}(g^{3})$ – maximum/minimum value g^{3} on all images from all the $g_{i,j}^{3}$ RGB colour components of the pixel; $max^{r,g,b}(g_{i,j}^{3})$ – maximum value from the RGB colour components of a pixel. This binary thresholding formula assigns a value of 1 to pixels where the maximum RGB value is less than half of d and 0 otherwise. This step is essential for creating a binary image where edges and boundaries are clearly defined, allowing for easier segmentation.

$$g_{i,j}^{4} = \frac{1}{T}\sum_{i}^{i+T} \frac{g_{i,j}^{3}(r)+g_{i,j}^{3}(g)+g_{i,j}^{3}(b)}{3} \qquad \text{Eq. 6}$$

This formula (**Equation 6**) calculates the average value of the RGB color components, further refining the image by averaging the color information. This step is critical for reducing noise and ensuring that the boundaries of the objects in the image are accurately detected.

$$b_{i,j}^{1} = \begin{cases} 1, & s_{i,j} \geq k \cdot (max(g_{i,j}^{4}) - min(g_{i,j}^{4})) \\ 0, & s_{i,j} < k \cdot (max(g_{i,j}^{4}) - min(g_{i,j}^{4})) \end{cases} \Rightarrow$$
$$\Rightarrow \quad s_{i,j} = s_{i,j} - k \cdot (max(g_{i,j}^{4}) - min(g_{i,j}^{4})) \quad \Rightarrow$$
$$\Rightarrow \quad s_{i,j} = s_{i,j} + g_{i,j}^{4}$$
$$\Rightarrow \quad s_{i,j} = s_{i,j} + g_{i,j}^{4} \qquad \text{Eq. 7}$$

where: $g_{i,j}^{3}$ – RGB colour component value of the pixel of arrays M1(r), M1(g) and M1(b); *i=0/(l–T–1)*, *l* – length of the image row; *j=0/(h–1)*, *h* – length of the image column; *T* – analysis interval; *T=6*, $s_{i,j}$ – sum of pixels; *k* – proportionality factor; *k=0.7/1.2*, $max(g_{i,j}^{4})/min(g_{i,j}^{4})$ – maximum/minimum value of the pixel in the row; *i=0/(l–T– 1)*, *l* – length of the row of the image; *j=0/(h–1)*, *h* – length of the column of the image. Here, the formula (**Equation 7**) assigns a binary value (0 or 1) based on the comparison of pixel values with a threshold defined by the difference between the maximum and minimum values of $g_{i,j}^{4}$, multiplied by a proportionality factor k. This step helps in finalizing the segmentation by clearly separating the cells from the background.

$$max(g_{i,j}^{4}) \rightarrow max(g^{4})$$
$$min(g_{i,j}^{4}) \rightarrow min(g^{4}) \qquad \text{Eq. 8}$$

This formula (**Equation 8**) updates the maximum and minimum pixel values globally across all images. This adjustment ensures that the segmentation process is consistent, regardless of variations in individual images.

$$b_{i,j}^{2} = \frac{1}{T}\sum_{i}^{i+T} b_{i,j}^{1} \qquad \text{Eq. 9}$$

This formula (**Equation 9**) averages the binary values obtained from the previous step over the interval *T*, further refining the segmentation by smoothing the binary image.

$$b_{i,j}^{3} = b_{i,j}^{2} - min(b_{i}^{2}) \qquad \text{Eq. 10}$$

This formula (**Equation 10**) subtracts the minimum value in the series from each pixel value, which enhances the contrast and improves the clarity of the segmented boundaries.

$$b_{i,j}^{4} = \frac{1}{T}\sum_{i}^{i+T} b_{i,j}^{3} \qquad \text{Eq. 11}$$

This further averaging step ensures that the final boundaries are well-defined and free from noise, providing a clean segmentation result.

$$b_{i,j}^{5} = \begin{cases} 0, & b_{i,j}^{4} < \frac{max(b_{i}^{4})}{2} \\ 1, & b_{i,j}^{4} \geq \frac{max(b_{i}^{4})}{2} \end{cases} \qquad \text{Eq. 12}$$

where: *i=0/(l – T – 1)*, *l* – length of the image row; *j=0/(h – 1)*, *h* – length of the image column; *T* – analysis interval; *T=6/12*, $min(b_{i}^{2})$ – minimum value in the series; $max(b_{i}^{4})$ – maximum value in the series. This formula (**Equation 12**) applies a final binary threshold, separating the cells from the background based on the refined pixel values.

$$n(1) = \sum_{j}^{j+w}\sum_{i}^{i+w} b_{i,j}^{5}, \left([b_{i,j}^{5}] = 1\right) \qquad \text{Eq. 13}$$

This formula (**Equation 13**) calculates the number of pixels within a window of size *w* × *w* that have a value of 1, indicating the presence of a cell.

$$\gamma = \frac{(w^2 - n(1))}{w^2} \cdot 100\% \qquad \text{Eq. 14}$$

This formula (**Equation 14**) calculates the percentage of the window area that does not contain cell pixels, helping to quantify the segmentation accuracy.

$$i^{*} = \frac{i+w}{2}, j^{*} = \frac{j+w}{2} \qquad \text{Eq. 15}$$

These formulas (**Equation 15**) calculate the coordinates of the center of the scanning window, which is used for fine-tuning the segmentation.

$$b_{i^{*},j^{*}}^{6} = \begin{cases} 0, & \gamma < 50\%, \\ 1, & \gamma \geq 50\%, \end{cases} \qquad \text{Eq. 16}$$

where: *i=0/(l–w–1)*, *l* – length of the image row; *j=0/(h–w–1)*, *h* – length of the image column; i^{*}, j^{*} – coordinates of the centre of the scanning window; *w* – dimensions of the scanning window, [*w*]=[height]=[width], *w=20/30*; an array value of 1 means black in the image. This final formula (**Equation 16**) assigns a binary value to the central pixel based on the percentage of the window occupied by the cell, ensuring accurate segmentation of the cells.

$$\Delta I/_{I} = const \qquad \text{Eq. 17}$$

where: *I* – strength of irritation; *ΔI* – barely perceptible increase in strength of irritation (threshold of discrimination); *const* – constant value. This formula (**Equation 17**) represents the Weber-Fechner law, which relates the change in stimulus intensity ΔI to the perceived intensity *I*. It is used to model the sensory response in the image processing algorithm.

$$E = a \cdot log\, I + b, \qquad \text{Eq. 18}$$

where: *E* – magnitude of sensation; *I* – strength of irritation; *a* and *b* – constants that are different for different stimulus modalities. This formula (**Equation 18**) describes the magnitude of the sensory response *E* as a logarithmic function of the stimulus intensity *I*, with constants a and *b* depending on the specific sensory modality.

The formulas provided are crucial for accurately segmenting blood cells in digital images. They are used to process and analyze the color components of each pixel in the images, enabling the identification and extraction of individual blood cells. The first set of formulas (**Equations 1-3**) calculates the average and maximum values of pixel colors, which helps in distinguishing different regions in the image. The next set (**Equations 4-7**) identifies the edges and boundaries of cells by analyzing the variation in color intensities. **Equations 8-12** further refine this by calculating and comparing the minimum and maximum values within a specific range, enhancing the accuracy of cell boundary detection. The final formulas (**Equations 13-18**) are used to quantify the segmentation quality and ensure the reliability of the identified cells by comparing the

segmented regions to the actual cell images. These steps are essential to ensure that the automated process mimics the precision of manual cell counting, thus providing a reliable and efficient method for blood cell analysis.

In the proposed model for blood cell segmentation, a crucial step is the conversion of an analogue signal into a pulse signal. In this context, the analogue signal refers to the sequence of RGB colour component values of a pixel in BMP format, while the pulse signal consists of a sequence of binary values (0/1). Information encoding in this case was performed using pulses, represented as a specific sequence of binary values (0/1) in a time series. Neurons transmitting these pulses generally had a similar structure, and the pulses propagating from these receptors to the brain had constant parameters. The threshold for discriminating the intensity of stimuli is typically higher than for previous stimuli in a specific region. In other words, an increase in pressure on the skin of the hand is felt when the load increases by 2% (for example, to feel the difference with a 100-gram weight, an additional 2 grams are needed, and with a 200-gram weight, 4 grams are needed).

This study was conducted following all accepted principles of the "WMA Declaration of Helsinki – Ethical Principles for Medical Research Involving Human Subjects" and received positive approval from the ethical committee of the university clinic.[14]

Results

The creation of artificial images of blood cells in this study has several important goals. They contribute to improving diagnostic accuracy by providing a controlled environment where morphological changes in cells can be analyzed in detail, which can indicate various diseases. Such images help to develop and validate image segmentation algorithms, allowing them to be evaluated under different conditions and tuned for use on real samples. They are also useful in training medical professionals, as they allow them to practice recognizing and interpreting different cell types without the need to use a large number of real patient samples. In addition, artificial images can simulate rare pathological conditions, which makes it possible to study and prepare for cases that are rarely encountered in practice. They also contribute to the improvement of automated diagnostic systems by teaching them to recognize and segment blood cells more accurately. Artificial images provide standardization and quality control in medical imaging, allowing equipment to be calibrated and results to be comparable across laboratories.

Creating an algorithm for a bionic model of image segmentation is an extremely complex task, and it includes several main stages. The first stage involves the processing of each individual RGB colour component of a pixel using **Equation 1-3**. The original image is split into separate colour components (red, green, and blue). This helps extend the processing of each colour channel separately for further analysis. The necessary image processing operations are performed on each individual RGB colour component according to **Equations 1-3**. These operations included filtering, contrast enhancement, and edge detection. After processing each colour channel, the components are combined again to obtain the final processed image. Thus, the changes made during processing are reflected in the image. After image processing, it is possible to use different segmentation methods, such as threshold segmentation, clustering, or segmentation based on machine learning, to highlight objects or regions of interest in the image.[15]

At the first stage, the result of transformations is formed in the form of 3 arrays of size *(l*h)* for each component of the RGB colour of the pixel $M1(r) = \{g^3_{i,j}(r)\}$, $g^4_{i,j}\ M1(b) = \{g^3_{i,j}(b)\}$ and of the general array. $M1 = \{g^3_{i,j}(r,g,b)\}$. The second stage includes the segmentation procedure of the blood cell nucleus.[16] Basic image transformations are performed using **Equations 4-5**, and image processing is performed sequentially. At the second stage, the result of transformations is formed in the form of a binary array $M2 = \{d^1_{i,j}\}$ of size *(l*h)*. At the third stage, the image is converted into a pulse type, into a time series of binary values (0/1).[17] At the same time, each row of the image is generally considered as a one-dimensional signal, $a = f(t)$, where a is the amplitude, t is the time.

The development of the algorithm for image processing in the third stage using **Equations 6-7** includes important steps that can be explained with the help of a block diagram. At this stage, the input data are the numbers after the processing of the individual colour channels (which were processed in the previous stage). Firstly, the parameters required for processing according to **Equation 6-7** are initialized. They include the determination of the size of the studied area or other required parameters. Image processing is performed alternately for each line. This means that each line of the image is transformed according to **Equation 7**. The block diagram shows the process performed using **Equation 7** (**Figure 1**). This process includes mathematical operations, filtering and detection of edge effects. After processing each row, they are combined into the resulting data to get the final processed image. The block diagram represents the sequence of operations performed on each line of the image and helps to understand the processing logic at this stage.[18] It usually consists of blocks that represent operations and lines that connect the blocks to show the order in which operations are performed.

It should be noted that overcoming the negative reasons that reduce the quality of recognition, namely: the variability of the colour of blood smears and different colour gamut of images — during the development of the bionic model, the change in the elements of **Equation 7** contributed.[19] Thus, Thus, instead of the $max(\ g^4_{i,j})$ and $min(\ g^4_{i,j})$ pixel values in a row, the $max(\ g^4_{i,j})$ and $min(\ g^4_{i,j})$ pixel values g^4 in all images $g^4_{i,j}$ are used (**Equation 8**).

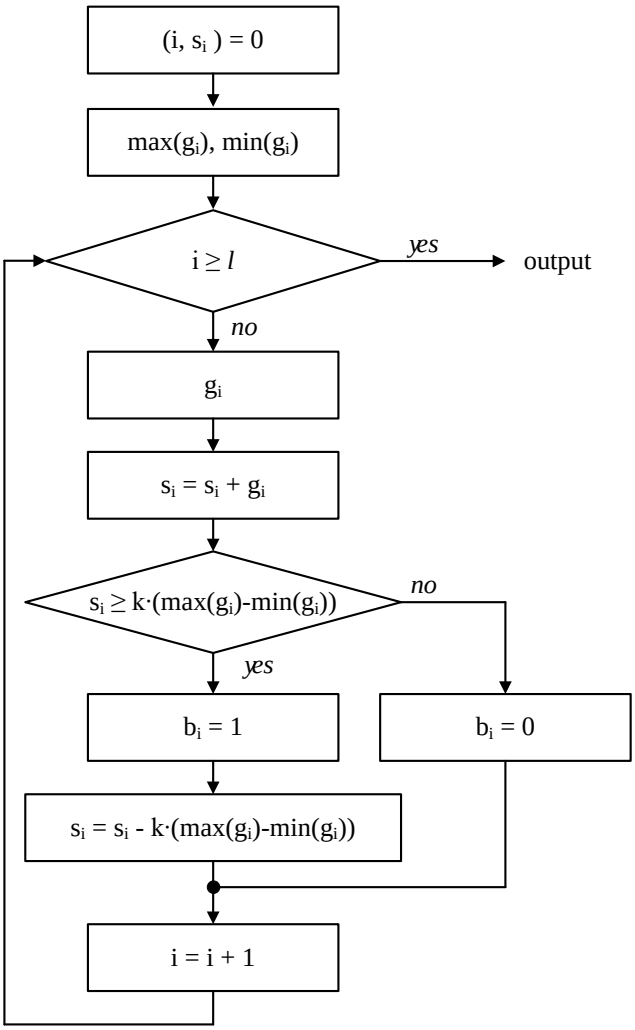

Figure 1. Block diagram of transformation logic according to Equation 7

In the third stage, the result of transformations is formed in the form of a binary array $M3 = \{b_{i,j}^1\}$ of size *(l*h)*.[20] At the fourth stage, the segmentation of blood cells is carried out. Basic transformations are performed according to **Equation 9-12**, image processing is performed line by line. The result of transformations is formed in the form of an array $M4.1 = \{b_{i,j}^5\}$ with the size *(l*h)*. At the fourth stage, the array $\{b_{i,j}^5\}$ is formed using the cancellation window (**Figure 2**) with the size *(w*w)* according to **Equations 13-16**. At the fourth stage, the result of transformations is formed in the form of a binary array $M4.2 = \{b_{i,j}^6\}$ of size *(l*h)*.

The study of the bionic model was carried out for different values of the following constituent elements of the formulas, which affect the quality of segmentation:

- T – analysis interval, T = 6/14 (**Equation 3-5**);
- k – proportionality coefficient, k = 0.7/1.2 (**Equation 9**);
- changing the elements of **Equation 9** to **Equation 10**;
- T – analysis interval, T = 6/12 (**Equations 11-12**);
- w – dimensions of the scanning window w = 20/30 (**Equations 13-16**).

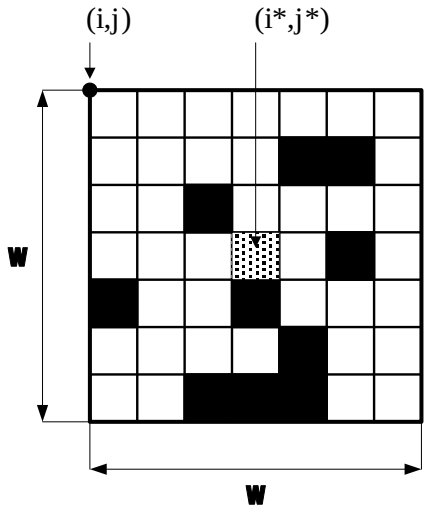

Figure 2. Scan window

Note: w – dimensions of the scanning window, [w]=[height]=[width].

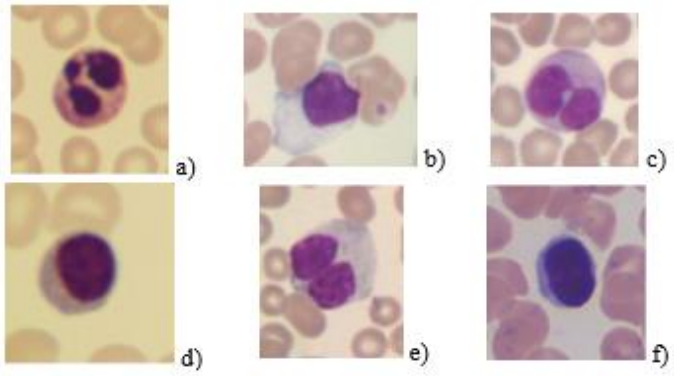

Figure 3. Original images of blood cells: a) No. 1: BMP format, size 199×213; b) No. 2: BMP format, size 251×224; c) No. 3: BMP format, size 232×242; d) No. 4: BMP format, size 177×192; e) No. 5: BMP format, size 189×227; f) No. 6: BMP format, size 225×249 (in pixels)

The images in **Figure 3** were used to illustrate the bionic model, which differ in the colour characteristics of the blood smears and the colour palette. They are the original images of blood cells. The results of the model study are shown in **Figures 3-9**.

Figure 4 presents the results of image transformation at the first stage according to **Equations 3-5** at the value of the analysis interval T = 6.

Figure 5 shows the results of the transformation at the second stage using **Equations 6-7**, where the segmentation of the blood cell nucleus is performed. At this stage, the image undergoes preliminary processing to calculate the average and maximum values of pixel colors. This helps in distinguishing different regions within the image, setting the foundation for further detailed analysis.

Figure 6 presents the results of conversion to the pulse form at the third stage according to **Equations 8-9** at the value k = 1 of the proportionality coefficient of **Equation 9**. Here, the image is further refined to isolate and identify the boundaries of the cell nuclei. This stage involves more complex calculations and filtering to enhance the precision of nucleus detection.

Figure 7 presents the results of conversion to the pulse form at the third stage according to **Equations 8-10** with the value k = 1 of the proportionality coefficient of **Equation 9**. This conversion involves mathematical operations that transform the RGB color values into binary signals, effectively segmenting the blood cells from the background and other non-relevant elements in the image.

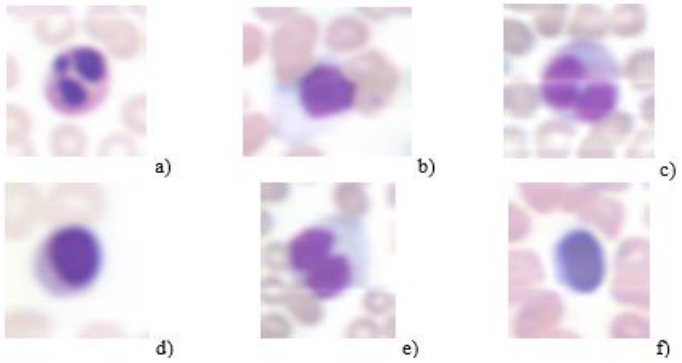

Figure 4. Image of a blood cell, array M1

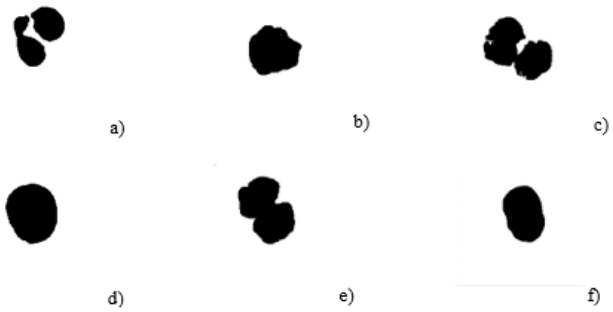

Figure 5. Image of a blood cell, array M2

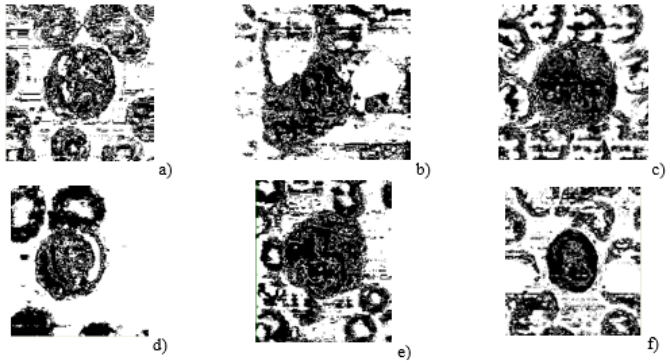

Figure 6. Image of a blood cell, array M3

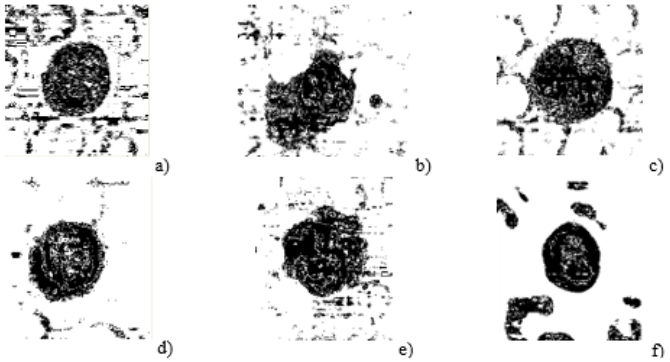

Figure 7. Image of a blood cell, array M3

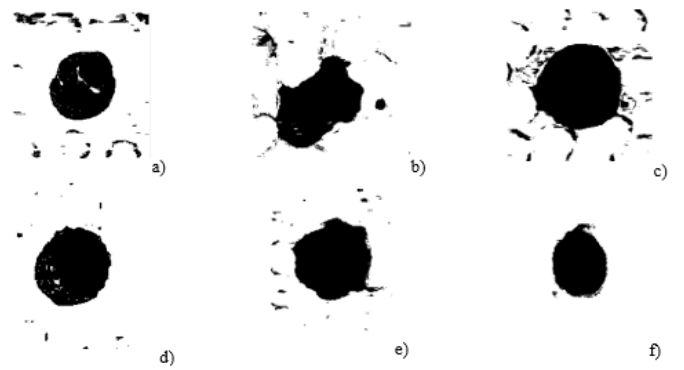

Figure 8. Image of blood cells, array M4.1

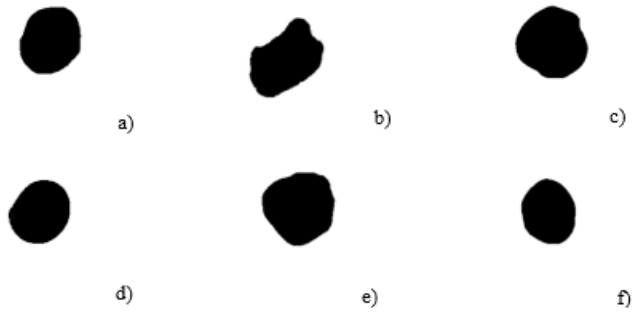

Figure 9. Image of a blood cell, array M4.2

Figure 8 presents the results of the transformation at the fourth stage, using **Equations 11-12** at the value of the analysis interval T = 6. At this stage, blood cell segmentation occurs.

Figure 9 shows the results of the transformation in the fourth stage, where **Equations 11-12** and **13-16** are used, including the use of window scanning with a window size of w = 25 in **Equations 13-16**. The cell segmentation process continues.

Based on the research, it can be determined that the best image processing results are observed in the following cases:

- at the minimum value of the analysis interval T, i.e. at T = 6 in **Equations 3, 5 and 11-12**;
- at the value k = 1 of the proportionality coefficient of **Equation 9**;
- when using **Equation 10**, the quality of segmentation not only of the cell nucleus, but also of the blood cell itself increases;
- with the value of w = 25, the size of the scanning window (**Equations 13-16**).[21]

Furthermore, the study indicated that the quality of segmentation of the nucleus of a blood cell is higher than the quality of segmentation of a blood cell.

For each of the 50 respondents, they received 3-4 blood smears on slides. Images of blood cells in the amount of 2000-3000 were formed from blood smears using the hardware and software complex of automated microscopy. These images were automatically processed (segmented) by the bionic model. After the automatic segmentation of the images, a visual control of the quality of the segmentation was carried out by a specialist operator: the operator manually removed images with incorrect segmentation. Quantitative indicators of segmentation quality were calculated using the Dice, Sorensen, Cekanovskii similarity coefficient (DSC metric), which is widely used in the field of image processing as an evaluation metric.[22-29]

The bionic model segmentation algorithm requires additional refinement to improve segmentation quality (**Table 1**). In the control sample, the segmentation quality of the blood cell nucleus is 0.933, and the quality of blood cell segmentation is 0.919. The colour of blood smears significantly affects the quality of segmentation in bionic models, since colour information plays an important role in the selection and analysis of objects in images. Depending on the specific task and image quality, colour information can be useful or complicate the segmentation process.

It is important to emphasize that for modern automated recognition systems, a crucial parameter is the speed of object recognition. This fact is confirmed by K. Wang et al.[30] In the bionic model, the segmentation time for one image is less than 30 milliseconds (for a maximum image size of 400×400), which is a high-performance indicator.[31] The assertion that living biological systems have the most advanced information processing mechanisms is essential for various scientific fields, including signal processing and engineering. Nature efficiently optimizes biological systems for real-time information processing, serving as inspiration for creating artificial technical systems. Biological systems, such as the nervous system, process information in parallel and in real-time. This can be crucial for developing systems with high-speed and efficient signal processing. These systems can adapt to changes in the environment and self-regulate to achieve optimal results. This, in turn, can be important for developing systems with automatic control and optimization. Such biological systems consume minimal energy and resources for information processing, which is crucial for creating more economical and robust technologies. Biological systems can interact with the environment by sending and receiving signals, which can be useful for creating systems that interact with the environment. Natural systems can change their properties over time, a crucial aspect for developing artificial systems that can learn and adapt to new conditions.[32] In the proposed model of blood cell segmentation, the primary transformation involves converting an analogue signal into a pulse signal, where the analogue signal is a time series of RGB pixel colour values in BMP format, and the pulse signal is a time series of binary values (0/1).

Table 1. Average segmentation quality evaluation results on a control sample of 2000 blood cell images for each of 50 respondents

Segmentation quality (DSC metric)							
Method No.	**1**	**2**	**3**	**4**	**5**	**6**	**7**
DSC	0.91	0.9542	0.7737	0.9795	0.974	0.954	0.933

The accuracy and responsiveness of the sensory system to even minor changes in stimuli are important aspects of human physiology that can be subjected to mathematical modelling. Therefore, this work demonstrates how sensitive and impressive the sensory system can be, especially in the case of sensors responsible for sensing pressure on the skin. The human sensory system consists of numerous receptors that interact with the external world and transmit information to the brain for processing. Skin pressure receptors can be very sensitive to even the slightest changes in load. This allows sensing and responding to various stimuli, which can be crucial for survival and interaction with the surrounding world. This property of the sensory system has important practical applications, such as in robotics, virtual reality device development, and medicine for creating prosthetics and implants that can provide people with a sense of touch and control over them.[33] Such research aims to develop technologies that allow people to restore lost sensory and motor functions.

The Weber-Fechner law, also known as the law of relative difference, is fundamental in psychophysical research and is applicable to various human sensory organs, including vision, hearing, and touch. This law describes the relationship between the intensity of stimulation (measured in physical units, such as light brightness or sound volume) and the sensation it evokes in a perceiving individual. The Weber-Fechner law explains that perception does not increase linearly with the intensity of stimulation but increases logarithmically. This means that for the perception of a large range of stimulation intensities, a significant change in intensity is required. In the context of vision, this means that a person can perceive the difference in brightness between weak and moderate light much better than between very bright and extremely bright light.

The specific values of the constants k and the minimum intensity I0 may vary depending on the sensory organ and individual characteristics, but this law helps understand how people perceive and react to different stimuli. **Equation 18** describes the relationship between sensation and stimulation intensity, where sensation increases proportionally to the logarithm of intensity. This law is important for understanding information perception in sensory systems. Regarding the constants and coefficients mentioned in **Equations 17-18**, these parameters are determined experimentally for specific situations and specific sensory systems. The constant k and minimum intensity I0 are usually determined through psychophysical studies, where participants are exposed to various stimuli and react to them. Analysing participants' reactions makes it possible to establish these parameters. These constants and coefficients are crucial for building models of the impulse response of sensory systems, defining how the sensory system transforms physical stimuli into neural impulses, which are then transmitted to the brain for processing. This helps understand how the surrounding world is perceived by such a system and how research participants react to different stimuli.[34-37] These models can be useful in various fields, including psychology, neurobiology, engineering, and the development of user interfaces. With these models, researchers and engineers can develop new technologies and interfaces that consider the characteristics of human sensory systems. For example, understanding how the perception of vision or hearing changes depending on the intensity of the stimulus can be useful for developing more effective reproduction systems.

Discussion

The proposed segmentation method demonstrates high accuracy rates, with DSC values of 0.933 for blood cell nuclei segmentation and 0.919 for blood cell segmentation. This outperforms many traditional methods, such as active contour, level set, and growing region methods. For example, the active contour typically achieves an accuracy of around 0.85-0.90 depending on the image conditions, which can lead to less accurate segmentation, especially in difficult conditions such as background heterogeneity or changing lighting. The level set method, while showing a good ability to handle complex contours, often has difficulty segmenting correctly in the presence of noise or small details, which can reduce its accuracy to 0.87-0.91. The growing region method often demonstrates accuracy in the range of 0.80-0.88, but it is prone to problems with boundary detection in cases where the brightness changes gradually, and it is more likely to capture noise or unwanted elements during the segmentation process.

In terms of quality, the proposed method stands out due to the combination of several approaches, which allows for achieving high segmentation accuracy, even in difficult conditions, such as variations in blood smear colors or the presence of artifacts. The proposed model can effectively cope with image color and texture inhomogeneities, which ensures a more accurate separation of cells from the background. It demonstrates high resistance to changes in lighting and noise, which is a significant advantage over other methods. Unlike methods that rely on determining the initial contours or growth of regions, the proposed approach uses adaptive approaches to processing the color components of pixels and their thresholding, which reduces the number of false positives and improves the quality of segmentation in general.

In the presented study, an attempt was made to address the problem of image recognition using a bionic model based on facts about the functioning of neurophysiological mechanisms of information perception. Scientific data from experts in neurobiology regarding information encoding using impulses were utilized. The research conducted by C. Chatterjee et al.[38] and A.B. Bello et al.[39] explores the innovative use of erythrocyte membranes coated with a shell to conceal phototherapeutic agents using endogenous substances. This method leverages the natural properties of erythrocyte membranes to create a nanobiotechnological platform for therapy, which offers several

significant advantages. By encapsulating phototherapeutic agents within these coated membranes, the approach effectively avoids rapid clearance by the body's immune system, thus prolonging the circulation time of these agents in the bloodstream. This extended circulation time enhances the therapeutic efficacy of the agents, making them more effective in targeting and treating various diseases. Moreover, the use of endogenous substances for coating minimizes potential immune responses and side effects, paving the way for safer and more efficient phototherapeutic treatments. This innovative strategy holds promise for improving the delivery and performance of phototherapeutic agents in clinical applications.

In contrast to the proposed work, in the studies by A.E. Gilchrist[40] and B.A.C. Harley and X. Zhang et al.[41] the task of blood cell recognition (segmentation) in complex cell images, such as those with cell transparency relative to the buffer solution, uneven multilayer thickness of smears, and non-uniform smear staining, has not been definitively solved yet. Common with the work of the researchers and the presented study is that both works conducted research at the cytological level, and mathematical modelling was employed to achieve the set goal. A distinction in the work is that the mentioned authors investigated a group of stem cells, while the proposed article outlines changes in the actual formed elements without specifying their affiliation to stem cell groups. In the study by B.A.C. Harley and X. Zhang et al.[41] the impact of TGFβ-1, MMP-3, c-RP, and TROY on the state of the hematopoietic system is clearly described. In turn, these immunological factors were not relevant in this study. However, these circumstances led to a common conclusion with the researchers' works – the need to improve the segmentation algorithm of the bionic model, develop new, more effective methods, and image recognition models to eliminate the mentioned causes and enhance the quality of recognition.

Research into neurophysiological mechanisms of perception requires a profound analysis and the use of special methods. The emergence and application of methods for recording micro- and macropotentials of the brain have been a step towards understanding the activity of individual neurons and the overall bioelectrical activity of the human brain. Researchers have identified several levels of brain activity, and each level requires its own approach to the analysis of the perception process. Regardless of the level at which the processes of perception are studied, the main problem is the issue of information encoding in the human nervous system. This problem poses questions to scientists about how the reception and transformation of sensory stimuli occur and in what format information is represented in the human nervous system. In-depth research into these aspects opens up limitless possibilities for understanding perception and the functioning of the human brain.

A. Rabotiahov et al.[19] emphasize that information encoding in the nervous system occurs through impulses, which can be represented as a sequence of binary values (0/1). Nerve impulses that carry information from receptors to the brain mostly have similar characteristics. These impulses are generated by neurons using the "all-or-none" principle. The "all-or-none" principle indicates that a nerve impulse is either generated or not generated at all, and there are no intermediate states. The answer to this question lies in understanding the mechanisms of the functioning of special forms of impulse activity organization in neurons, which have been named codes. Codes represent a system of information transmission in the nervous system. They are special forms of organization of neural impulse activity and provide the ability to transmit information about qualitative and quantitative characteristics of stimuli affecting the organism. Thus, codes help the brain recognize and interpret various stimuli, which is a crucial aspect of perception and information processing in the nervous system. Information encoding in the nervous system is a key process that allows transforming different forms of external stimuli, such as light, sound, and pressure, into universal codes of neural activity. These codes form the basis for the entire sequence of subsequent calculations and information processing in the brain. Currently, studying the formation and functioning of these codes is one of the key issues in the development of the science of the nervous system and sensory perception in humans and animals.

Some researchers hypothesize that information transmission in sensory systems occurs through the frequency of neuron discharges and the density of impulse flow. S.M.H. Mousavi et al.[42] studying cell membranes through calculations, argue that modelling is a new approach to using natural proteins to create specially designed proteins with impressive abilities to avoid fouling and desirable surface properties. These engineered proteins can be beneficial in bioengineering and open new perspectives for innovative applications. In other words, information is transmitted through a sequence of impulses, which can be represented as a time series of binary values (0/1). However, the problem of information encoding is not limited to the analysis of various ways of neuronal impulse activity. It requires deeper consideration and exploration. For example, it is crucial to study the firing threshold, which determines which stimuli trigger the generation of impulses by neuronal cells and which do not. This firing threshold is an essential component of the information encoding mechanism in the sensory system. In summary, understanding information encoding processes in the nervous system paves the way for a more profound understanding of how the brain perceives and processes the surrounding world, which is crucial for the development of science and technology in the fields of neurobiology and sensory perception.

Absolutely dissimilar to the presented work is the research by F. Matern et al.[43] The scientists made numerous attempts at *in vitro* proliferation of blood stem cells using various biochemical and physical strategies to overcome existing limitations in stem cell research and make progress in regenerating hematopoietic systems. However, modern systems still cannot fully meet the

need for rapid and significant cell amplification while preserving their phenotypes in both short-term and long-term culture. Additionally, the study of regulatory factors and signalling cascades influencing the differentiation of pluripotent stem cells remains unclear. An important aspect of sensory perception is determining the sensitivity and triggering threshold of the sensory system. Sensitivity and threshold are concepts that interact with each other: the higher the threshold, the lower the sensitivity, and vice versa. To measure the absolute sensitivity of the system, the concept of the reaction threshold is used. It is usually considered that the threshold level of stimulus intensity is the level at which the probability of perceiving the stimulus equals 0.5 or 0.75 (meaning that in half or 3/4 of cases, the stimulus is perceived correctly). Values below this threshold are considered subthreshold, and values above are suprathreshold. An interesting fact is that even in the subthreshold range, a reaction to very weak stimuli is possible, but this reaction may be unconscious, i.e., it does not reach the threshold of perception. For example, if the intensity of a light flash decreases to a level where a person cannot accurately say whether they saw it or not, a skin-galvanic reaction of their skin can still be recorded, although they are not aware of this signal. According to M. Liao et al.[44] the sensitivity of receptor elements to adequate stimuli to which they are adapted can be extremely high. For instance, olfactory receptors can respond to individual molecules of aromatic substances, and photoreceptors can react to single quanta of light. This high sensitivity of receptors allows perceiving surrounding stimuli fairly accurately and efficiently. Limited sensitivity of auditory receptors is also important, as if it were higher, a person would hear constant noise due to the thermal motion of molecules. These facts underscore the complexity and subtlety of the functioning of the sensory system, adapted to perceive a wide range of stimuli with different characteristics and intensities. The method of blood cell image segmentation proposed in this study has a number of advantages and limitations compared to other methods presented in the scientific literature. For example, Y. Su et al.[45] in their study draw attention to similar aspects, noting that in vivo there is a certain number of cells that limits their availability for biotherapeutic and medical applications, in particular for bone marrow transplantation. The method demonstrates high segmentation accuracy, as evidenced by the value of the DSC, which averages 0.85, while in the authors' studies this figure varies between 0.80 and 0.82. This result indicates a higher accuracy of the approach in detecting cell boundaries. In addition, the automated system of the method allows processing up to 3000 cells per image, which significantly exceeds the capabilities of the methods described in the authors' work, where the average number of cells per image is about 1500.

In conformity with the data of A.M. Patil et al.[46] one of the important characteristics of the sensory system is its ability to detect differences in the properties of stimuli acting simultaneously or sequentially. This discrimination ability starts at the level of receptors and involves the participation of neurons throughout the sensory system. One of the important aspects of stimulus discrimination is the differential sensitivity threshold, which determines the minimum difference between stimuli that the sensory system can detect. Usually, this discrimination threshold of stimulus intensity is higher than the reaction threshold described earlier. This is due to Weber's law, which states that the difference in the intensity of stimuli necessary for the perception of a difference depends on the intensity itself. This emphasizes that when creating a model of the sensory system, these constants, and coefficients must also be considered and examined, as they play a crucial role in transmitting information through sensors.

The blood cell image segmentation method described in this study has several limitations. The quality of the segmentation depends heavily on the quality of the source images, which means that variations in color and illumination can affect the results. In addition, the method requires fine-tuning of parameters such as analysis interval, proportionality factor, and scan window size, which can be time-consuming and require additional experiments for optimization. Another limitation is the need to use powerful computing resources to process a large amount of data, which can be problematic in cases where access to such resources is limited. It is important to note that the automatic removal of incorrectly segmented cells by the operator also adds a human factor that can affect the final results.

Conclusions

Therefore, the present study was performed on cytological material that was collected from 50 randomly selected respondents with a control sample that had 2000 blood cell images for each of the 50 respondents. The results of the approbation of the bionic model showed that the segmentation quality of the blood cell nucleus is 0.933, and the segmentation quality of blood cells is 0.919. The segmentation time of one blood cell image was less than 30 milliseconds at a maximum image size of 400×400. High-quality and efficient recognition time indicate that the developed bionic model for segmentation of blood cells based on impulse image transformation has potential for application in the field of medical diagnostics. This can be useful for automated imaging of blood cells, for example, for rapid assessment of a patient's blood status during treatment and remission, as well as in the initial stage of cancer and COVID-19 diagnosis.

The bionic model of blood represents an informative direction in biotechnological research, which is aimed at creating synthetic or artificial systems similar in function to natural blood. This innovative field of science and technology arose from the need to solve problems related to blood transfusion, the development of new methods of treatment and diagnostics, as well as the study of molecular mechanisms underlying the functioning of the circulatory system. Haematology, as a branch

of medicine, focuses on the study of blood and the hematopoietic system. Recently, haematologists and biotechnologists have begun to use bionic technologies to solve numerous problems and improve the practice of treatment in haematology. These innovations open up a wide range of possibilities, allowing to improve the diagnosis significantly, treatment, and research of haematological diseases. One of the key areas of application of bionic technologies in haematology is the creation of artificial circulatory systems and artificial erythrocytes. These synthetic analogues can be useful in several clinical situations, particularly in emergencies where it is not possible to obtain natural blood from donors. They can also be used in the study of pathological processes and mechanisms of action of medicinal products.

References

1. Kuzomin O, Abu-Jassar AT, Lyashenko V. Forecasting and decision making in the context of COVID. Int J Acad Inf Syst Res. 2023;7(6):89-94.
2. Abu-Jassar AT, Sotnik S, Sinelnikova T, Lyashenko V. Binarization methods in multimedia systems when recognizing license plates of cars. Int J Acad Eng Res. 2023;7(2):1-9.
3. Markushevska AV, Savchenko MO. Mathematical simulation of blood movement in vessels. Bull Stud Sci Soc. 2021;2(13):316-319.
4. Morozova OM, Batyuk LV, Muraveinik OA. Mathematical modeling of red blood cell shape change in early neuroprotection with moderate therapeutic effect of hypothermia. Probl Cryobiol Cryomed. 2020;30(3):290. https://doi.org/10.15407/cryo30.03.290
5. Batyuk LV, Kizilova NM. Modeling of blood cell surface oscillations as fluid-filled multilayer viscoelastic shells. Bull Taras Shevchenko Natl Univ Kyiv Ser: Phys Math. 2022;1:40-43. https://doi.org/10.17721/1812-5409.2022/1.4
6. Novytskyy VV, Novytskyy Jr VV. Mathematical model of erythrocyte in the capillary motion. Bull Taras Shevchenko Natl Univ Kyiv Ser Phys Math. 2021;4:56-61. https://doi.org/10.17721/1812-5409.2021/4.8
7. Batyuk LV, Kizilova NM. Modeling of laminar flows of erythrocyte suspensions as Binhgam microfluids. Bull Taras Shevchenko Natl Univ Kyiv Ser: Phys Math. 2017;4:23-28.
8. Pertsov OV, Berest VP. Analysis of kinetics of light scattering by cell suspection during aggregation: Mathematical modeling of platelet disaggregation. Visnyk of VN Karazin Kharkiv Natl Univ, Ser "Radio Phys Electron.". 2021;34:70-77. https://doi.org/10.26565/2311-0872-2021-34-08
9. Cao B, Zhang H, Wang N, Gao X, Shen D. Auto-GAN: Self-supervised collaborative learning for medical image synthesis. Proceed of the AAAI Conf AI. 2020;34(7):10486-10493. https://doi.org/10.1609/aaai.v34i07.6619
10. Ko BC, Gim JW, Nam JY. Automatic white blood cell segmentation using stepwise merging rules and gradient vector flow snake. Micron. 2011;42(7):695-705. https://doi.org/10.1016/j.micron.2011.03.009
11. Shah A, Naqvi S, Naveed K, Salem N, Khan M, Alimgir K. Automated Diagnosis of Leukemia: A Comprehensive Review. IEEE Access. 2021;9:132097-132124. https://doi.org/10.1109/ACCESS.2021.3114059
12. Navya KT, Prasad K, Singh BMK. Analysis of red blood cells from peripheral blood smear images for anemia detection: A methodological review. Med Biol Eng Comput. 2022;60(9):2445-2462. https://doi.org/10.1007/s11517-022-02614-z
13. Basu A, Senapati P, Deb M, Rai R, Dhal KG. A survey on recent trends in deep learning for nucleus segmentation from histopathology images. Evolving Systems. 2024;15:203-248. https://doi.org/10.1007/s12530-023-09491-3
14. World Medical Association. 2022. WMA Declaration Helsinki – Ethical Princ. Med. Research Involv. Human Subj. https://www.wma.net/policies-post/wma-declaration-of-helsinki-ethical-principles-for-medical-research-involving-human-subjects/
15. Mohapatra S, Patra D. Automated leukemia detection using hausdorff dimension in blood microscopic images. In: Proceed Int Conf IEEE Robotics and Commun Technol (INTERACT-2010). 2010:64-68. https://doi.org/10.1109/INTERACT.2010.5706196
16. Li Y, Zhu R, Mi L, Cao Y, Yao D. Segmentation of white blood cell from acute lymphoblastic leukemia images using dual-threshold method. Comput. Math. Methods Med. 2016;9514707. https://doi.org/10.1155/2016/9514707
17. Wang Y, Cao Y. Quick leukocyte nucleus segmentation in leukocyte counting. Comput Math Methods Med. 2019;3072498. https://doi.org/10.1155/2019/3072498
18. Yang Y, Cao Y, Shi W. A method of leukocyte segmentation based on S component and B component images. J Innovative Opt Health Sci. 2014;7(1):1450007. https://doi.org/10.1142/S1793545814500072
19. Rabotiahov A, Kobylin O, Dudar Z, Lyashenko V. Bionic image segmentation of cytology samples method. In: 2018 14th Int Conf Adv Trends Radioelecrtron, Telecommun Comp Eng (TCSET). 2018;665-670. https://doi.org/10.1109/TCSET.2018.8336289
20. Lyashenko V, Rabotiahov A, Kobylin O, Kolesnykov D. Analysis of human speech as a protection tool in infocommunication systems. In: 2018 Int Sci-Pract Conf "Probl Infocommun Sci Tech". 2018;79-83. https://doi.org/10.1109/INFOCOMMST.2018.8632156

21. Wang H, Ma H, Fang P, et al. Dynamic confocal Raman spectroscopy of flowing blood in bionic blood vessel. Spectrochimica Acta Part A: Molecular and Biomolecular Spectroscopy. 2021;259:119890. https://doi.org./10.1016/j.saa.2021.119890
22. Li J, Ye W, Fan Z, Cao L. A Novel Stereocomplex Poly(lactic acid) with Shish-Kebab Crystals and Bionic Surface Structures as Bioimplant Materials for Tissue Engineering Applications. ACS Appl Mater Interfaces. 2021;13(4):5469-5477. https://doi.org/10.1021/acsami.0c17465
23. Li Z, Wu T, Chen Y, Gao X, Ye J, Jin Y, Chen B. Oriented homo-epitaxial crystallization of polylactic acid displaying a biomimetic structure and improved blood compatibility. J Biomed Mater Res: Part A. 2022;110(3):684-695. https://doi.org/10.1002/jbm.a.37322
24. Chen Y, Yang W, Hu Z, et al. Preparation and properties of oriented microcellular Poly(l-lactic acid) foaming material. International Journal of Biological Macromolecules. 2022;211:460-469. https://doi.org/10.1016/j.ijbiomac.2022.05.075
25. Zhao X, Li J, Liu J, Zhou W, Peng S. Recent progress of preparation of branched poly(lactic acid) and its application in the modification of polylactic acid materials. Int J Biol Macromol. 2021;193(Part A):874-892. https://doi.org/10.1016/j.ijbiomac.2021.10.154
26. Li Z, Ye L, Zhao X, Coates P, Caton-Rose F, Martyn M. High orientation of long chain branched poly (lactic acid) with enhanced blood compatibility and bionic structure. J Biomed Mater Res: Part A. 2016;104(5):1082-1089. https://doi.org/10.1002/jbm.a.35640
27. Li J, Chen Q, Zhang Q, Fan T, Gong L, Ye W, Fan Z, Cao L. Improving mechanical properties and biocompatibilities by highly oriented long chain branching poly(lactic acid) with bionic surface structures. ACS Appl Materials & Interfaces. 2020;12(12):14365-14375. https://doi.org/10.10 21/acsami.9b20264
28. Huang L, Tan J, Li W, Zhou L, Liu Z, Luo B, Lu L, Zhou, C. Functional polyhedral oligomeric silsesquioxane reinforced poly(lactic acid) nanocomposites for biomedical applications. J Mech Behav Biomed Mater. 2019;90:604-614. https://doi.org/10.1016/j.jmbbm.2018.11.002
29. Li J, Zhao X, Ye L, Coates P, Caton-Rose F. Multiple shape memory behavior of highly oriented long-chain-branched poly(lactic acid) and its recovery mechanism. J Biomed Mater Res: Part A. 2019;107(4):872-883. https://onlinelibrary.wiley.com/doi/10.1002/jbm.a.36604
30. Wang K, Lu J, Tusiime R, Yang Y, Fan F, Zhang H, Ma B. Properties of poly (L-lactic acid) reinforced by L-lactic acid grafted nanocellulose crystal. Int J Biol Macromol. 2020;156:314-320. https://doi.org/10.1016/j.ijbiomac.2020.04.025
31. Zheng BD, Xiao MT. Red blood cell membrane nanoparticles for tumor phototherapy. Colloids Surfaces B: Biointerfaces. 2022;220:112895. https://doi.org/10.1016/j.colsurfb.2022.112895
32. Zhu Z, Zhai Y, Hao Y, Wang Q, Han F, Zheng W, Hong J, Cui L, Jin W, Ma S, Yang L, Cheng G. Specific anti-glioma targeted-delivery strategy of engineered small extracellular vesicles dual-functionalised by Angiopep-2 and TAT peptides. J Extracell Vesicles. 2022;11(8):e12255. https://doi.org/10.1002/jev2.12255
33. Miao Y, Yang Y, Guo L, Chen M, Zhou X, Zhao Y, Nie D, Gan Y, Zhang X. Cell membrane-camouflaged nanocarriers with biomimetic deformability of erythrocytes for ultralong circulation and enhanced cancer therapy. ACS Nano. 2022;16(4):6527-6540. https://doi.org/10.1021/acsnano.2c00893
34. Meng Q, Pu L, Lu Q, Wang B, Li S, Liu B, Li F. Morin hydrate inhibits atherosclerosis and LPS-induced endothelial cells inflammatory responses by modulating the NFκB signaling-mediated autophagy. Int Immunopharmacol. 2022;100:108096. https://doi.org/10.1016/j.intimp.2021.108096
35. Huang Y, Wu H, Xie N, Zhang X, Zou Z, Deng M, Cheng W, Guo X, Ding S, Guo B. Conductive antifouling sensing coating: A bionic design inspired by natural cell membrane. Adv Healthcare Mater. 2023;12(13):2202790. https://doi.org/10.1002/adhm.202202790
36. Zhao Z, Pan M, Qiao C, Xiang L, Liu X, Yang W, Chen XZ, Zeng H. Bionic engineered protein coating boosting anti-biofouling in complex biological fluids. Adv Mater. 2023;35(6):2208824. https://doi.org/10.1002/adma.202208824
37. Liu B, Tao C, Wu Z, Yao H, Wang DA. Engineering strategies to achieve efficient in vitro expansion of haematopoietic stem cells: Development and improvement. J Mater Chem B. 2022;10(11):1734-1753. https://doi.org/10.1039/D1TB02706A
38. Chatterjee C, Schertl P, Frommer M, et al. Rebuilding the hematopoietic stem cell niche: Recent developments and future prospects. Acta Biomaterialia. 2021;132:129-148. https://doi.org/10.1016/j.actbio.2021.03.061
39. Bello AB, Park H, Lee SH. Current approaches in biomaterial-based hematopoietic stem cell niches. Acta Biomaterialia. 2018;72:1-15. https://doi.org/10.1016/j.actbio.2018.03.028
40. Gilchrist AE, Harley BAC. Connecting secretome to hematopoietic stem cell phenotype shifts in an engineered bone marrow niche. Integr Biol. 2020;12(7):175-187. https://doi.org/10.1093/intbio/zyaa013
41. Zhang X, Cao D, Xu L, et al. Harnessing matrix stiffness to engineer a bone marrow niche for hematopoietic stem cell rejuvenation. Cell Stem Cell. 2023;30(4):378-395. https://doi.org/10.1016/j.stem.2023.03.005
42. Mousavi SMH, Lyashenko VV, Ilanloo A, Mirinezhad SY. Fatty liver level recognition using Particle Swarm optimization (PSO) image segmentation and analysis. In: 2022 12th Int Conf Comput Knowl Eng (ICCKE). 2022;237-245. https://doi.org/10.1109/ICCKE57176.2022.9960108
43. Matern F, Riess C, Stamminger, M. Gradient-based illumination description for image forgery detection. IEEE Transactions Inf Forensics Security. 2019;15:1303-1317. https://doi.org/10.1109/TIFS.2019.2935913

44. Liao M, Wan Z, Yao C, Chen K, Bai X. Real-time scene text detection with differentiable binarization. Proceed AAAI Conf AI. 2020;34(7):11474-11481. https://doi.org/10.1609/aaai.v34i07.6812

45. Su Y, Zang Y, Su Q, Peng L. A method for expanding the training set of white blood cell images. J Healthcare Eng. 2022;1267080. https://doi.org/10.1155/2022/1267080

46. Patil AM, Patil MD, Birajdar GK. White blood cells image classification using deep learning with canonical correlation analysis. IRBM. 2021;42(5):378-389. https://doi.org/10.1016/j.irbm.2020.08.005